Far Field, Near Field and SAR Simulation for Cell Phones Operating Close to the Head

Mateus Bonadiman, Claudio R. Fernández and Álvaro A. de Salles

Electrical Engineering Dept., Federal University of Rio Grande do Sul (UFRGS), Brazil

Abstract — **The Finite-Difference Time-Domain (FDTD) method to calculate the cellular phone far and near field and the specific absorption rate (SAR) in the user's head is described. The conventional λ/4 monopole and a simple planar antenna are simulated. A multidimensional grid is developed to optimize simulations in the near and in the far field, in the presence and in the absence of the cellular phone user's head at 1.9 *GHz*. These calculations show that significant improvement in the antenna radiation efficiency and in the reduction of the SAR in the head are obtained when planar antennas are used.**

Index Terms — **Finite-Difference Time-Domain (FDTD), Specific Absorption Rate (SAR), Cellular Phone, Biological Effects, Planar Antennas.**

I. INTRODUCTION

The use of mobile phone in professional and private activities has grown substantially in the last years. In parallel with this, an increased concern has been demonstrated by the scientific community, the authorities and the population regarding the safety of these phones, since they employ monopole or whip antennas operated very close to the user's head. This results in a high Specific Absorption Rate (SAR) in the head tissues. Also, in that situation the radiation performance of these antennas are modified, e.g., in terms of input impedance, radiation pattern and radiation efficiency. This results in poor communication quality and an increase in the battery drain.

The Finite Difference Time-Domain (FDTD) method has been used by several authors to simulate the Specific Absorption Rate (SAR) in the user's head [1-9]. It is currently the most appropriate choice when highly non-homogeneous structures are involved for which other numerical methods (such as boundary techniques) have fundamental limitations. However, the grid used by most authors for the discretisation has fixed dimensions in all the space of simulation. This is adequate to simulate the SAR in the head, but it would result in a waste of processing time and in the use of exaggerated memory resources, if the calculation of the far field were desired.

The authors are with the Optoelectronic Communications Laboratory, Electrical Engineering Department, UFRGS, Av. Osvaldo Aranha, 103, Porto Alegre, 90.035-190, RS, Brazil, Tel. + 55-51-33163517, Fax. + 55-51-33163293. M. Bonadiman, mbonad@iee.ufrgs.br; C. Fernández, fdez@iee.ufrgs.br and A. A. de Salles, aasalles@vortex.ufrgs.br.

The simulation of the far field can be relevant for systems design and for the simulation of its performance. Furthermore, it can be an important tool for the design and simulation of new devices producing lower SAR in the head and improving systems performance, such as planar antennas with optimised radiation pattern.

In this work, the FDTD method with a multidimensional grid is used to calculate the near field, the SAR in the head and the far field (with and without the presence of the head) for two antennas, the monopole and a simple microstrip antenna. The advantages of this method and the benefits of planar antennas in comparison with the conventional monopole antennas are discussed.

The maximum mean power delivered (P_{del}) by cellular phones is now in the range of 125 or 250 *mW* when operating in digital mode, and in the range of 600 *mW* when operating in analogue mode. When the digital phones are in roaming, they operate in the analogue mode. Therefore, in the simulations, P_{del} = 600 *mW* was used, since this is the worst situation. The simulation was performed at frequencies close to 1.9 *GHz* , since in this range more results from other authors were available for comparison, and since this frequency band was recently authorised for the operation of new cellular phones in our country.

II. THE FDTD METHOD WITH A MULTIDIMENSIONAL GRID

In order to allow an adequate representation of the different biological tissues in the head and details of the antenna, the mesh should be small in comparison to the wavelength. Then, an available neuro-anatomical data base [10] was used to generate a discrete model of the human head with cubic cells having Δ=1.8 *mm* [8]. This was denominated "thin mesh region". The domain had also another region named "coarse mesh region", in which the cells have Δ_g = 27 *mm*, at a distance greater than 10λ from the antenna, and where the far field and the radiation pattern of the two antennas were calculated. Fig. 1 shows a domain composed of two meshes with different dimensions. Since Δ_g is 15 times greater than Δ, then the calculations in the coarse mesh are updated at intervals of 15 times longer than those for thin mesh.

The dimensions used in the thin mesh are $23.04 \times 30.60 \times 32.40$ *cm*, ($128\Delta \times 170\Delta \times 180\Delta$), and $3.51 \times 3.645 \times 4.59$ *m* ($130\Delta_g \times 135\Delta_g \times 170\Delta_g$) for the coarse mesh. The absorbing wall described by Mur [11] was used as the boundary condition.
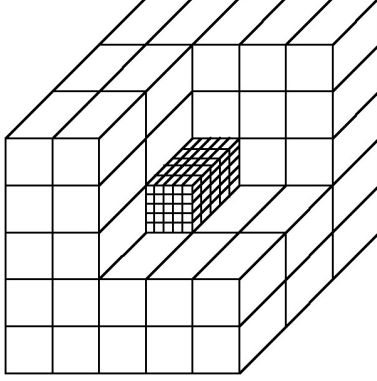

Fig. 1. A domain composed of two meshes with different dimensions (multidimensional grid).

III. SIMULATION

Since the cells for the digitalisation of the head have a fixed length Δ, then all elements in this domain have dimensions defined as integer multiples of Δ. Therefore, the dimensions of the two antennas simulated are defined in terms of this value Δ. Also, in the simulation, the distance between the cellular phone and the head is 0.54 *cm* (3Δ), which is very close to the typical distance of operation.

The total time for each simulation in the *Cray T94* supercomputer was around 2 hours (this includes queuing time, waiting for the required CPU to be available), using 820 *MB* of memory. The total number of interactions was 2,400. Then, for a time differential of $\Delta t = 3.00208$ *ps*, used in the thin mesh, results a simulated time of 7.205 *ns*.

A. Model for the user head

The discretisation used for the head (generation of the mesh for the domain) has been described in previous works [5,6,8]. The head dimensions are shown in Fig. 2.
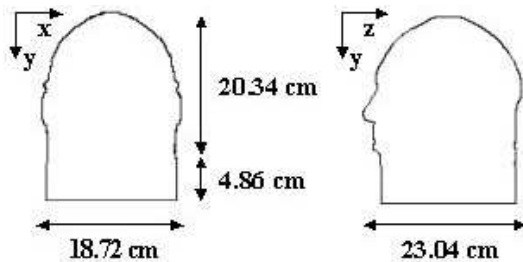

Fig. 2. Dimensions for the head model.

The different materials included in the head model were defined in accordance with the physical and electrical parameters for the different tissues close to 1.9 *GHz* [2,7], and are indicated in Table I.

TABLE I
PROPERTIES OF THE TISSUES USED IN THE FDTD SIMULATION AT
FREQUENCIES CLOSE TO 1.9 *GHz*

Tissue	ε_r	σ [mho/m]	ρ [Kg/l]
Skin/Fat	36.5	0.700	1.10
Muscle	55.3	2.000	1.04
Bone	7.75	0.105	1.85
Brain	46.0	1.650	1.03
Eye	80.0	1.900	1.02

B. Simulation of the $\lambda/4$ Monopole Antenna

The cellular phone was modelled as a metallic box (perfect conductor), covered with a 1.8 *mm* thick dielectric coating ($\varepsilon_r = 2.1$) [12], having external dimensions $45 \times 19.8 \times 117$ *mm* ($25\Delta \times 11\Delta \times 65\Delta$). The monopole antenna was modelled by a $\lambda/4$ metallic cylinder fixed on the top of the metal box as it is shown in Fig. 3. Since all dimensions are multiple of Δ, we defined a frequency of 1.8926 *GHz* and then $\lambda/4$ is a length of 39.6 *mm* (22Δ).

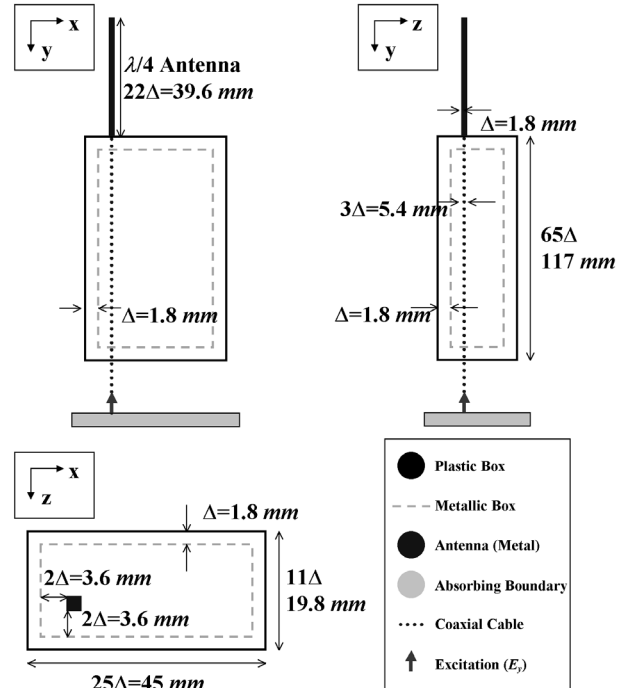

Fig. 3. Cellular phone with the $\lambda/4$ monopole antenna (fed through a coaxial cable).

The antenna feeding is supplied trough a coaxial cable, where the forced fields (E_y) are immediately above the absorbing wall (on the bottom of the coaxial cable internal conductor, see Fig. 3). This minimises straight radiation

by the power supply. However, since this excitation is not directly in the input of the antenna, a time delay due to the propagation in the coaxial cable must be considered. This time delay is $300\Delta t$, compared to the simulation of the microstrip antenna.

C. Simulation of the Microstrip Antenna

A simple rectangular patch microstrip antenna was chosen since its characteristics (e. g., radiation pattern) are convenient for this application and because its design procedure is well established [13]. In Fig. 4 the cellular phone model with the microstrip antenna located at its back face is shown.
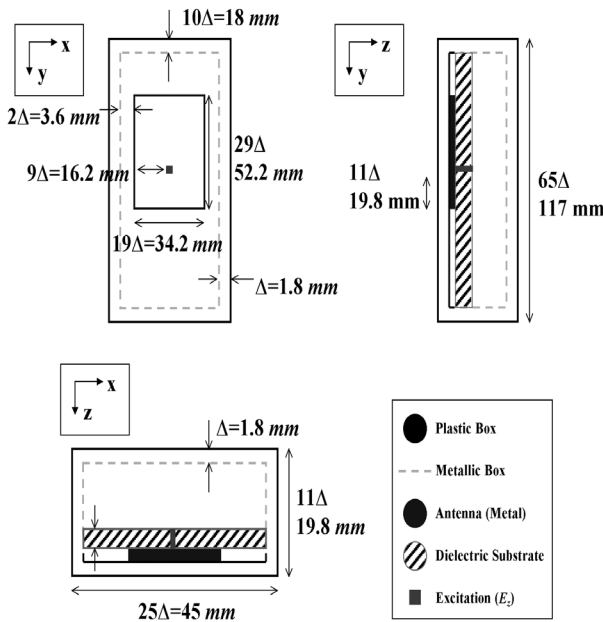

Fig. 4. Cellular phone with the microstrip antenna fed through a 1.8 mm diameter coaxial probe.

The substrate used has the same characteristics as the *RT/duroid 5880* [14] (ε_r = 2.2, $tg\delta$ = 0.0009 and h = 3.6 *mm*) and the internal conductor of the coaxial feeder has a 1.8 *mm* diameter.

The width of the antenna must be comparable (or smaller) with the cellular phone width (45 *mm* or 25 Δ) and with the dimensions of the cells of the mesh. Therefore a width W = 34.2 *mm* (19Δ) was used. For operation in the fundamental mode TM_{010} , then $L>W>h$. When the length L = 52.2 *mm* (29Δ), the resonance frequency is 1.862 *GHz*. Next, the distance y_o necessary for the central conductor of the coaxial cable to penetrate in the metallisation in order to obtain an antenna input impedance of 50 *ohms* was calculated to be y_o = 19.8 *mm* (11Δ). In the simulation, the electric field E_z was forced in this point. The calculated 3 *dB* bandwidth is 13 *MHz*, which can be improved, as well as other performances

parameters (e.g., VSWR, losses, radiation pattern, etc) if an optimised design were used.

This antenna was also simulated using the software Ensemble (SV v. 2.0.57) [15]. For the parameters indicated above, a standing wave ratio (VSWR) of 1.192 was estimated in the input line (50 *ohms*).

IV. RESULTS IN THE NEAR FIELD REGION

Two alternatives for the SAR in a cellular phone user's head were compared in these simulations: a) using a $\lambda/4$ monopole antenna and b) using a rectangular patch antenna. The field distribution in the domain was observed, as well as the SAR distribution in the head tissues when the two antennas were used. This is shown in Fig. 5 to 8.

In Fig. 5 and 6 the electric field intensity ($20\times\log|E|$) in frontal section (xy) (in the plane of the monopole antenna) and coronal section (in the bottom of the monopole antenna) respectively, are shown for both antennas (left: $\lambda/4$ monopole and right microstrip antenna). It can be observed that the fields in the brain are substantially reduced (more than 10 *dB*) when microstrip antennas are used, as it was already observed [2].

In Fig. 7 and 8 the SAR distributions in *dB* ($10\times\log[SAR]$) in the head are shown for the same frontal and coronal planes. These SAR values are normalised for a mean power delivered to the antenna equal to P_{del} = 600 *mW*, where 0 *dB* corresponds to a SAR = 1 *mW/g*. Again, it can be observed that the SAR levels in the head when the planar antenna is used are at least 10 *dB* lower than those estimated with the monopole. In the ICNIRP Guidelines [16], also provisionally recommended by the brazilian agency ANATEL [17], a maximum limitation of SAR = 2 *mW/g* is indicated. It can be observed that, under the simulation conditions, when the monopole antenna is used, this limit is substantially violated. These results are in accordance to those published by several authors [1-4,7,9]. However, as it has been shown in previous papers [5,6,8], if the monopole antenna where operated far from the head (e. g. at distances greater than 2.5 *cm*), then the ICNIRP Guidelines limit of SAR = 2 *mW/g* would be accomplished.

For the microstrip antenna, the reduction of field intensity and SAR in the head is substantial, and as a consequence of this, it is usually in compliance with the ICNIRP limit. Similar results with different directive antennas (e.g., planar antennas) where obtained by other authors [2,9].

As the power absorbed in the head (which is, together with the antenna losses, part of the total absorbed power P_{abs}) is reduced, an improvement in the radiation efficiency, η = $(P_{del} - P_{abs})/P_{del}$, for the planar antennas in comparison with the monopole antennas is obtained. This has been already described [2].
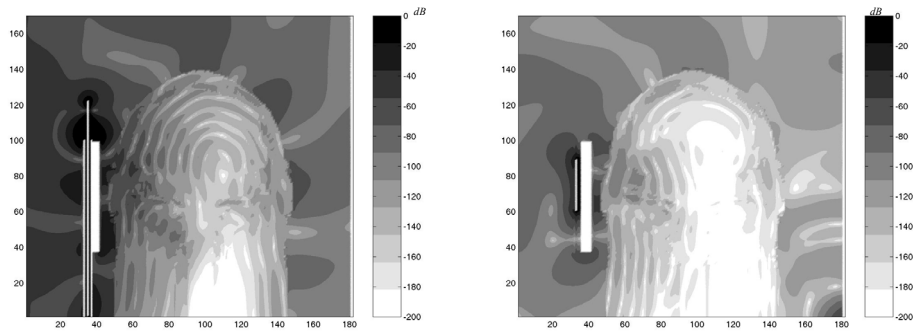
Fig. 5. Frontal images (*xy plane*) showing the electric field intensity (20×log|*E*|) obtained at the end of the simulations, left: λ/4 monopole and right: microstrip antenna.
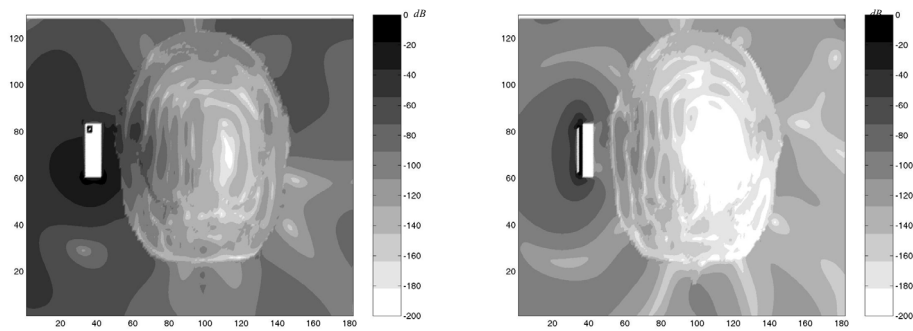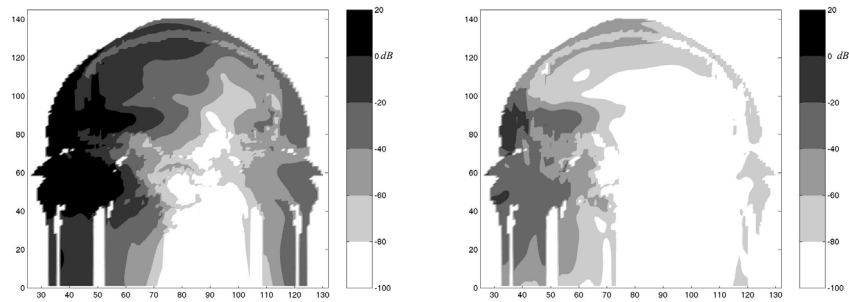

Fig. 6. Coronal images (*xz plane*) showing the electric field intensity (20×log|*E*|) obtained at the end of the simulations, left: λ/4 monopole and right: microstrip antenna.

Fig. 7. Frontal images (*xy plane*) of the SAR distribution [10×log(SAR)]. Left: λ/4 monopole and right: microstrip antenna. Cellular phone is at a distance of 0.54 *cm* and P_{del} = 600 *mW*. 0 *dB* corresponds to SAR = 1 *mW/g*.
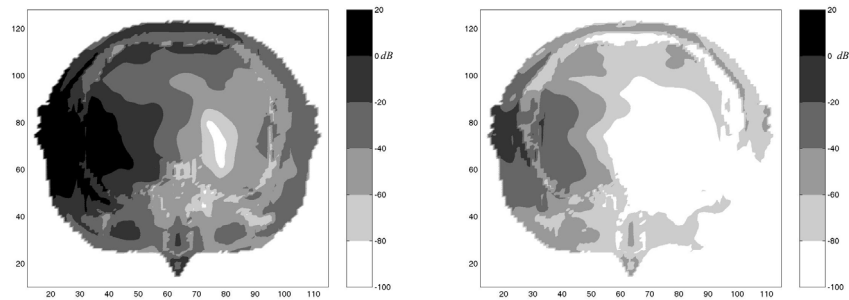

Fig. 8. Coronal images (*xz plane*) of the SAR distribution [10×log(SAR)]. Left: λ/4 monopole and right: microstrip antenna. Cellular phone is on the left of the head, at a distance of 0.54 *cm* and P_{del} = 600 *mW*. 0 *dB* corresponds to SAR = 1 *mW/g*.

V. RESULTS IN THE FAR FIELD REGION

The FDTD method with the coarse mesh was used to obtain the results in the far field region ($d \geq 10\lambda$), with and without the presence of the user's head, when the monopole antenna and when the microstrip antenna were used, at the frequency range of 1.9 *GHz*. The estimated radiation pattern in polar form at the horizontal plane are plotted in Fig. 9 to 11, for the monopole and for the microstrip antenna. Radial scale is 5 *dB*, and in order to simplify the comparison, the fields emitted from both antennas are normalised (made equal) in the direction opposed to the head.
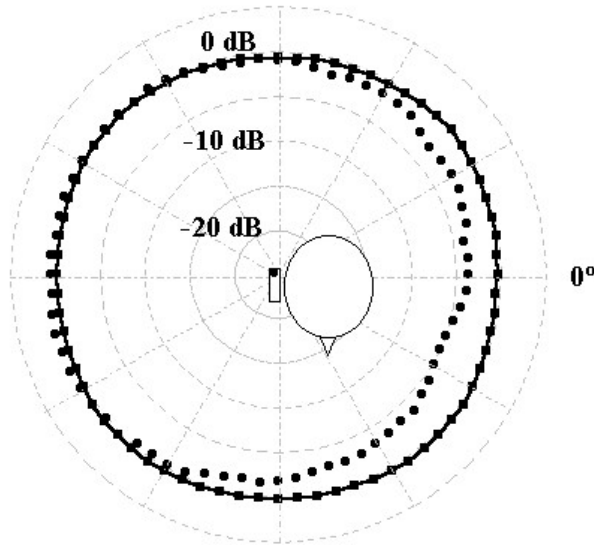

Fig. 9. Radiation Pattern (horizontal plane) for the λ/4 monopole antenna: continuous line (without head), dotted line (with the head).

In Fig. 9 the radiation patterns at the horizontal plane for the λ/4 monopole antenna with the presence of the head (dotted line) and without the head (continuous line) are shown. A reduction of around 5 *dB* in the direction including the user is observed due to the presence of the head. This is similar to the "Body Loss" values recommended by some authors in link design procedures [18,19].

An additional advantage of the FDTD method in comparison to other numerical methods is that the FDTD allows the simulation of the planar antenna without the requirement of infinite dimensions for the ground plane. As a consequence of this, a more realistic situation is simulated, and therefore the results should be more accurate.

In Fig 10, the radiation pattern without the presence of the head for the microstrip antenna (dotted line) is compared with that of the monopole antenna (continuous line). A front-to-back ratio in the range of 10 *dB* is observed for the microstrip antenna.
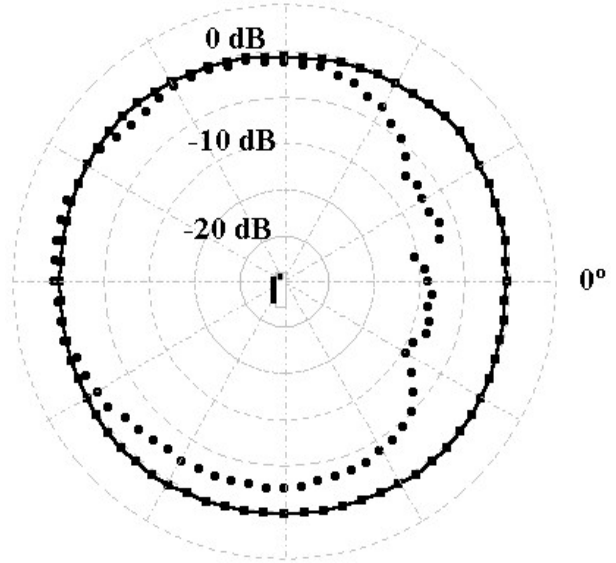

Fig. 10. Radiation Pattern (horizontal plane) without the head: continuous line (λ/4 monopole antenna), dotted line (microstrip antenna).

In Fig. 11, both antennas are compared when operating in the presence of the head. It can be observed that in the case of the microstrip antenna (dotted line), the front-to-back ratio is maintained a bit lower than 10 *dB*. Then, when a directive antenna (e.g., planar antennas) with low loss and low VSWR is used, obviously the energy emitted in the direction opposed to the head (which is the desired direction for communication) is improved in comparison with the use of conventional monopole antennas. This would result in an improvement of the link performance and in the quality of the communication.
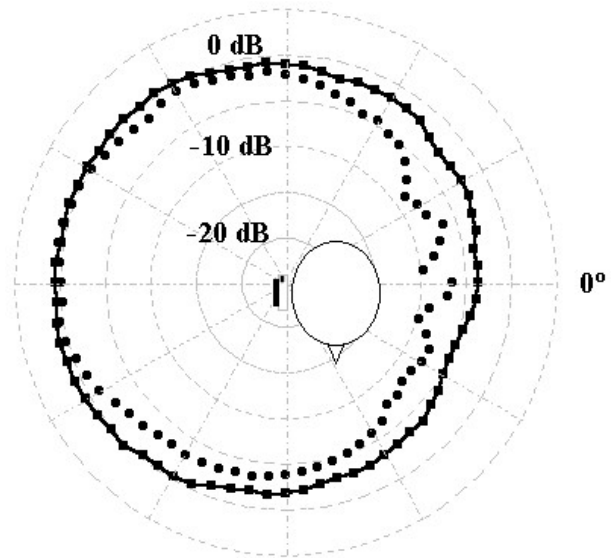

Fig. 11. Radiation Pattern (horizontal plane) including the head: continuous line (λ/4 monopole antenna), dotted line (microstrip antenna).

VI. Comments and Conclusions

The FDTD simulated results in the near field region (SAR) and in the far field region (radiation patterns) are shown in this work. This simulations were performed for two cases: with and without the presence of the user's head. Also, two different antennas were modeled: a usual monopole antenna and a simple rectangular patch microstrip antenna. The FDTD method with a multidimensional mesh was used. It was observed that the planar antenna has benefits both in terms of reduction of SAR in the user's head, as well as the improvement in the power emitted to the Radio Base Station with which it is communicating. Further to that, a reduction in the battery drain is expected.

The FDTD method is an important tool for the design of directive antennas for this application, showing adequate performance, among others, in terms of radiation pattern, VSWR, radiation efficiency and bandwidth.

The new generation of cellular phones (e.g. 2.5 G and 3 G) including services of message, voice, data, video, etc., will transmit higher data rates and may require higher transmitted power. This would result in greater risk for the cellular phone user unless alternatives such as directive antennas were employed. Hence, it is expected that these antennas, simple, compact and adequate for the integration with the cellular phone structure, with low cost and reasonable performance would perform an important function in the next generation of cellular phones.

Finally, it is important to remark that the usual guidelines for the human exposition limitations (e.g., ICNIRP) only consider the thermal effects of the non ionising radiation. If the non-thermal effects became definitively demonstrated, then the exposition limits will have to be substantially reduced. Therefore alternatives such as the planar antennas for mobile phones would become more relevant.

References

[1] P. J. Dimbylow and O. P. Gandhi, "Finite-Difference Time-Domain Calculations of SAR in a Realistic Heterogeneous Model of the Head for Plane-Wave Exposure from 600 MHz to 3 GHz", *Phys. Med. Biol.*, vol. 36, pp. 1075-1089, August 1991.

[2] M. A. Jensen and Y. Rahmat-Samii, "EM interaction of handset antennas and a human in personal communications", *Proc. of the IEEE*, vol. 83, nº. 1, pp. 7-17, January 1995.

[3] M. Okoniewski and M. A. Stuchly, "A study of the handset antenna and human body interaction", *IEEE T-MTT*, vol. 44, nº. 10, pp. 1855-1864, October 1996.

[4] S. Watanabe et al., "Characteristics of the SAR distributions in a head exposed to electromagnetic fields radiated by a hand-held portable radio", *IEEE T-MTT*, vol. 44, nº. 10, pp. 1874-1883, October 1996.

[5] A. A. Salles, C. R. Fernández e M. Bonadiman, "Simulação da Taxa de Absorção na Cabeça do Usuário do Telefone Celular", *anais do IX Simpósio Brasileiro de Microondas e Optoeletrônica*, pp. 473-477, Agosto 2000.

[6] A. A. Salles, C. R. Fernández e M. Bonadiman, "Distância da Antena e Potência Absorvida na Cabeça do Usuário de Telefone Celular", *anais do XVIII Simpósio Brasileiro de Telecomunicações*, Setembro 2000.

[7] M. F. Iskander et al., "Polarization and human body effects on the microwave absorption in a human head exposed to radiation from hand held devices", *IEEE T-MTT*, vol. 48, nº. 11, pp. 1979-1987, November 2000.

[8] A. A. Salles, C. R. Fernández e M. Bonadiman, "Distância da Antena e Potência Absorvida na Cabeça do Usuário de Telefone Celular Portátil", *Revista da Sociedade Brasileira de Telecomunicações*, vol. 16, nº. 1, pp. 16-28, Junho 2001.

[9] P. Bernardi et al., "Power absorption and temperature elevation induced in the human head by a dual-band monopole-helix antenna phone", *IEEE T-MTT*, vol. 49, nº. 12, pp. 2539-2546, December 2001.

[10] http://www.vhd.org.br.

[11] G. Mur, "Absorbing boundary conditions for the finite-difference approximation of the time-domain electromagnetic field equations", *IEEE Trans. Electomag. Compat.*, vol. 23, pp. 377-382, April 1981.

[12] K. Caputa et al., "Evaluation of electromagnetic interference from a cellular telephone with a hearing aid", *IEEE T-MTT*, vol. 48, nº. 11, pp. 2148-2154, November 2000.

[13] R. Garg, P. Bhartia, I. Bahl and A. Ittipiboon, *Microstrip Antenna Design Handbook*. Artech House, 2001.

[14] http://www.rogers-corp.com/mwu/.

[15] http://www.ansoft.com.

[16] ICNIRP Guidelines, *Guidelines for Limiting Exposure to Time-Varying Electric, Magnetic and Electromagnetic Fields (Up to 300 GHz)*, International Commission on Non-Ionizing Radiation Protection, "Health Physics", April 1998, vol. 74, nº. 4, pp. 494-522.

[17] ANATEL, *Diretrizes para Limitação da Exposição a Campos Elétricos, Magnéticos e Eletromagnéticos Variáveis no Tempo (até 300 GHz)*, aprovada pelo Conselho Diretor da ANATEL em 15 de Julho de 1999.

[18] H. Holma and A. Toskala, *Radio Access for Third Generation Mobile Communications*. John Wiley & Sons, 2000.

[19] J. Nielsen et al., "Statistics of measured body loss for mobile phones", *IEEE Trans. on AP*, vol. 49, nº. 9, pp. 1351-1353, September 2001.